

Statistics of Man-made Noise at 137 MHz

R. Dalke, R. Achatz, and Y. Lo
Institute for Telecommunication Sciences
Boulder, CO, 80303-3328

Abstract: Statistical noise models that simulate man-made noise are essential for the design of radio systems. Recently, the Institute for Telecommunication Sciences measured man-made VHF radio noise in the 136 to 138 MHz meteorological satellite band. These measurements were made as part of a link analysis for the broadcast of digital satellite weather images at 137 MHz. The measured noise statistics were used to develop analytical representations of the first-order probability distributions for man-made noise in various environments (business, residential, and rural). Such noise models are useful for simulating the performance of communications systems in environments where non-Gaussian man-made noise may degrade system performance. The statistical models as well as first-order probability distributions for several environments are presented in this paper.

INTRODUCTION

Man-made noise is an important consideration in the design and implementation of wireless communication systems. Typical sources of man-made noise in the VHF band include automobile ignition systems, electric motors, power systems, and a wide variety of electronic equipment such as computers and other commercial/consumer electronics devices. In 1974, Spaulding and Disney [1] presented results from many years of measurements of man-made radio noise. They devised methods for estimating the noise power and noise amplitude statistics that need to be accounted for in the design of radio systems. These methods are described in CCIR Reports [2] and have been widely used.

In recent papers, Spaulding [3, 4] warned that the CCIR methods for determining man-made noise levels may now be inaccurate due to technological advances. For example, newer automobile ignition systems radiate less noise, but the density of automobiles has increased dramatically. In addition, there has been a proliferation of electronic equipment that has become ubiquitous in business, residential, and rural environments. Thus, new procedures for measuring and modeling man-made noise are timely for understanding the environment in which communication systems operate.

The Institute for Telecommunication Sciences (ITS) recently completed an analysis of man-made noise at 137 MHz. The general methodology used to measure and analyze VHF noise statistics are described in [5, 6]. Our findings indicate that technological advances have significantly altered the noise environment from what is reported by the CCIR and that the

effects of man-made non-Gaussian noise should be considered in the design and implementation of VHF communication systems. An effective method for analyzing impulsive noise interference is to use statistical noise models in radio system simulations to evaluate the performance in non-Gaussian noise environments. In this paper we present statistical noise models that are based on the measured statistics of man-made noise at 137 MHz.

STATISTICAL-PHYSICAL PROBABILITY MODELS

Middleton [7-10] has published a detailed derivation of *Statistical-Physical models* of man-made and natural radio noise. Middleton's analysis of non-Gaussian noise is based on the assumption that the noise sources are Poisson distributed in space and time and that sources can have random amplitudes, durations, and frequencies. For the purposes of his analysis, Middleton divides the noise into three classes (A, B, and C; C being a combination of A and B) based on the interaction of the noise waveform and the receiver. Class A noise, while being impulsive in character, is defined as having a bandwidth that is smaller than the receiver filter of interest (the final IF filter for our purposes). With this assumption, the amplitude exceedence probability distribution (APD) of the received instantaneous power w is given by:

$$F_1(w) = e^{-\gamma T} \sum_{m=0}^{\infty} \frac{(\gamma T)^m}{m!} e^{-w^2/(2\sigma^2 \cdot m\beta^2)} \quad (1)$$

where γ is the mean pulse arrival rate, T is the mean pulse duration, $2\sigma^2$ is the mean power of the Gaussian component of the noise, and β^2 is the mean power in the received pulse. The APD does not depend explicitly on γ or T but their product and only three parameters are required. Furthermore, the average received power is roughly proportional to *impulse index* γT , hence the IF filter should not significantly affect the shape of the APD as long as its bandwidth is large when compared to the impulsive noise. It should be noted that when the noise bandwidth is extremely narrow, i.e., a *spectral line* source, the distribution is Nakagami-Rice as discussed later in this paper.

For Class B noise, the spectral width is much greater than the filter bandwidth. The resultant APD as calculated by Middleton consists of three components: a Gaussian component, an intermediate event component, and a rare event component. The rare event component has the same functional form as given in Equation 1. The intermediate component is much more complicated and includes an infinite series of confluent hypergeometric functions M :

$$F_2(w) = w \sum_{n=0}^{\infty} \frac{(-1)^n A_\beta^n}{n!} \Gamma(1 + \frac{\beta n}{2}) M(1 + \frac{\beta n}{2}, 2, -w) \quad (2)$$

where A_β is an "impulse index," and β is known as a spatial density-propagation parameter with the restriction $0 < \beta < 2$. In addition to the five parameters required for F_1 and F_2 , another parameter specifying the intersection point for the two functions must be used. Clearly, the implementation of Equation 2 in practical simulations is likely to be onerous. In addition, the determination and implementation of the required six parameters appears to be quite tedious and as noted by Hagn [11], practical parameter estimation techniques deserve considerable additional attention.

Our data represents the noise statistics after the noise process is filtered by the final 30-kHz IF filter in the measurement system. It is desirable that noise models be applicable in performance evaluations of communication systems having receiver bandwidths that differ from our measurement system; hence, the model should approximate the noise process as it would appear before passing through the measurement filter. Determining the parameters as required to fit Equation 2 to our measured statistical data does not really achieve this end. We did, however, use Middleton's results as a starting point in developing statistical noise models based on our measured data.

STATISTICAL NOISE MODELS BASED ON MEASUREMENTS

For a typical communication system, the received noise is *narrowband*, and hence, will be represented as a complex baseband function of time having a random envelope and phase. Following Middleton, we assumed that as observed by the receiver, the noise consisted of Poisson-distributed impulses plus a Gaussian component. In practice, two such Poisson processes were sometimes required to fit the measured data.

Class A Noise Model

Typically, Class A noise is characterized by a sudden jump in the APD curve when plotted on Rayleigh paper. Our measurements indicate that Class A events are rare, however, they did occasionally occur at many of our measurements sites. Usually, the total duration of these events was less than 100 ms. In most cases the amplitude is relatively large and the time between occurrences appears to be several hours.

An example of a measured and simulated APD showing expected Class A structure is shown in Figure 1. The APD's in this and following figures are plotted on Rayleigh paper and the amplitude is given relative to the thermal noise power in the receiver filter bandwidth, i.e., the product kT_0b where k is Boltzmann's constant, $T_0=290$ K, and b is the receiver bandwidth. As indicated previously, the simulated noise is

passed through a digital approximation of the final IF filter prior to calculating the APD.

In this example, Class A noise was simulated by generating pulses of 1 ms duration and constant amplitude. The pulse arrival times are Poisson distributed. For this simulation, the pulse arrival rate is 0.3/s and the amplitude is 67 dB. Class B noise was also included in this simulation. As noted earlier, only the product of the pulse duration and arrival rate can be determined from the APD. Additional measurements are required to determine the actual pulse duration.

Class B Noise Model

The Class B noise model consisted of Poisson distributed impulses with random amplitudes and phases plus complex Gaussian noise. A reasonable assumption for a narrowband system is that the phases are uniformly distributed. The remaining issue is the selection of an appropriate amplitude distribution function. We observe that when $w \gg 1$, the asymptotic expansion of the confluent hypergeometric function in Equation 2 yields [12]:

$$F_2(w) \approx \frac{1}{\pi} \sum_{n=0}^{\infty} \frac{(-1)^n}{n!} A_\beta^n \Gamma^2(\beta n) \beta n \sin(\pi \beta n) w^{-\beta n} \quad (3)$$

and when $\beta \ll 1$ and $A_\beta \ll 1$ so that only the first few terms of the series are important, the APD can be approximated using a Weibull distribution [13]:

$$F_2(w) \approx e^{-(w/w_0^2)^{1/\alpha}} \quad (4)$$

which is a generalization of the Rayleigh distribution. This distribution has a simple form which is commonly used and well adapted for simulating non-Gaussian noise (see e.g., [14]). The parameter α controls the slope of the APD when plotted on Rayleigh paper. This greatly simplifies the process of determining the appropriate value of the parameters. Also, the cumulative distribution function is easily inverted for use in Monte Carlo simulations. When the approximation is valid, the two parameters are directly related to Middleton's intermediate event impulsive index $w_0 = A_\beta^{-\alpha}$ and space density-propagation parameter $\alpha = 2/\beta$. Because of its merits, the Weibull distribution will be used in our analysis.

Specifically, the discrete Class B impulsive noise model used in our analysis consists of one or more independent sequences of independent events where the probability that k such events will happen in a particular time interval is Poisson. Each event is characterized by a random complex number with Weibull-distributed amplitude and uniformly distributed phase. To this we add complex Gaussian noise.

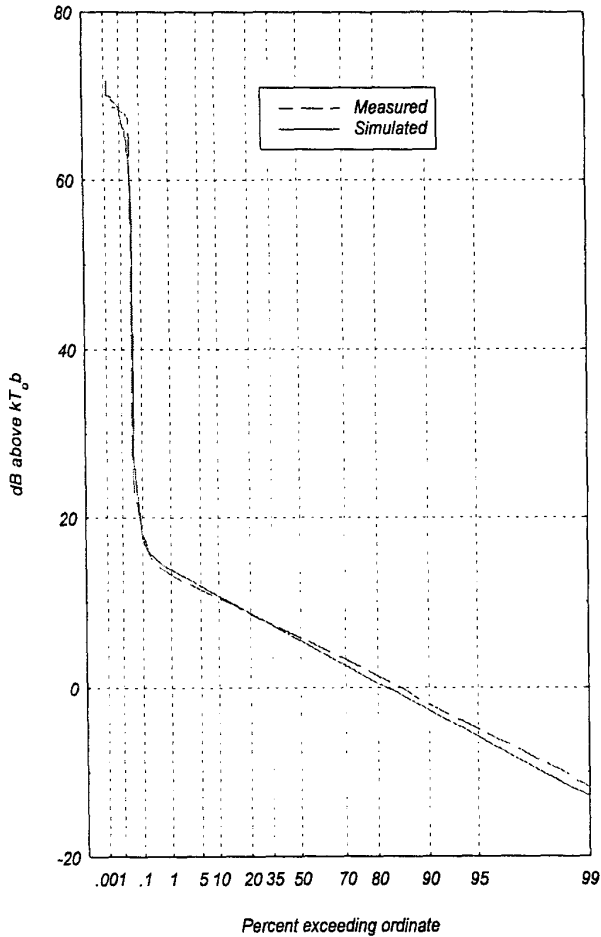


Figure 1. Distribution showing Class A noise characteristics.

The resultant discrete time series for the complex noise envelope can be expressed as follows:

$$v_k = (b_k \chi_k \cdot g_k) \xi_k \quad (5)$$

b_k is a Weibull variate:

$$b_k = \sqrt{w_o} (-\log_e u_k)^{\alpha/2} \quad (6)$$

χ_k is Poisson:

$$\chi_k = \begin{cases} 1 & \text{with probability } \lambda \Delta t \\ 0 & \text{with probability } \lambda \Delta t - 1 \end{cases} \quad (7)$$

where $0 \leq u_k \leq 1$ is a uniformly distributed variate, ξ_k is a complex sequence uniformly distributed on the unit circle, g_k is Rayleigh distributed, and Δt is the simulation time increment. This model

requires the determination of four parameters: the mean arrival rate λ , two Weibull parameters α and w_o , and the mean power in the complex Gaussian noise envelope w_{og} .

For most of our measurements, the mean power in the complex Gaussian noise envelope was readily estimated from the measured APD's. Ideally, the Weibull parameters α and w_o can be estimated from the slope and amplitude of the rarer events in the measured APD's. In practice, for many of the measured APD's, there was not sufficient rare event data to measure α accurately. In these cases, α was adjusted empirically to provide the best fit. The arrival rate is obtained from the probability associated with the point where the noise changes from Gaussian to non-Gaussian. This probability was estimated by assuming that the filtered noise pulse duration is equal to that of a rectangular pulse with approximately the same area as the impulse response of the filter.

Using the estimated parameters, a simulated noise time series was passed through a digital implementation of the six-pole Chebyshev IF filter used in the noise measurement system. The resultant APD was then compared with the measured APD. It was found that except for the mean power in the Gaussian component, a number of iterations are required to determine the optimum parameter values.

Spectral Line Source Noise Models

In some environments (e.g., business), *spectral line* sources of man-made noise were evident in addition to the typical Gaussian and impulsive noise sources. Possible sources of extremely narrowband noise are electronic equipment such as computers, switches, motors, and electrical distribution equipment (e.g., transformers). The sum of a *spectral line* source and Gaussian noise is characterized statistically by a Nakagami-Rice distribution which when plotted on Rayleigh paper has a slope that is greater than a Rayleigh distribution. The Nakagami-Rice probability density function is given by

$$f(w) = \frac{1}{w_{og}} e^{-(w+w_c)/w_{og}} I_0 \left(\frac{2\sqrt{w_c w}}{w_{og}} \right) \quad (8)$$

where I_0 is the modified Bessel function, w_c is the power in the *line source*, and w_{og} is the mean Gaussian noise power. The Nakagami-Rice distribution is commonly characterized by the parameter $K = 10 \log_{10}(w_c/w_{og})$. When both *line* sources and Class B impulsive noise sources are present, the noise model given in Equation 5 was modified by adding a constant power source to the complex Gaussian component.

COMPARISON OF MEASURED AND SIMULATED NOISE STATISTICS

Figures 2-4 show the measured and simulated APD's resulting from man-made noise near a noisy power line in a rural environment, in a downtown business district, and in an office

park near a major highway. These results are based on a digital simulation that uses a time increment of 10 μ s. The tacit assumption in our model is that prior to the final IF filter, Class B noise can be treated as a series of pulses having a duration of less than the time increment used in the digital simulation. The sampling increment selected for a particular receiver simulation would of course be based on the bandwidth of the receiver IF filter.

In Figure 4, the high exceedence probabilities are not Rayleigh distributed. At this location, it was conjectured that transformers or other electrical/electronic equipment may be sources of extremely narrowband noise and the resulting distribution is Nakagami-Rice.

Table 1. Simulation parameters for various noise environments.

Fig #	Noise environment or source	λ /s	α	w_0^* dB/kT	w_{0g} dB/kT
2	Rural: noisy power Line	495	0.5	46	5
3	Business: downtown	150	2.5	30	18
4	Business: office park	10	2.0	33	11

* w_0 depends on the time increment of the simulation.

Note that the simulated APD containing a *spectral line* component with the parameter $K=3$ dB is in good agreement with the measured APD lending strong support to this hypothesis.

In Figure 5 we give an example of a performance prediction for a digital communication system subjected to the man-made noise characterized by the APD shown in Figure 2. The figure shows the bit error ratio (BER) as a function of the signal-to-noise ratio (SNR) for a differentially coherent binary phase-shift keyed (DCBPSK) digitally modulated signal in an additive white-Gaussian noise (AWGN) channel compared with a communication channel receiving the power line noise. In this example, the power line severely degrades the performance of the digital transmission.

CONCLUSIONS

In this paper we have described analytical-statistical man-made noise models based on noise measurements at 137 MHz. Such models are important for use in performance evaluations of, for example, space-to-earth links operating in the 136 to 138 MHz meteorological band. The connection between our model and physically based statistical models such as those developed by Middleton is described. The model used in our work is much simpler than that presented by Middleton, having only four

parameters that can be estimated directly from the measured APD's. Furthermore, it is not restricted to the particular filter bandwidth used to obtain the measured data. Calculations using our statistical noise models are in good agreement with measurements, and we have found that, in general, the models provide a good representation of measured APD's.

REFERENCES

- [1] A.D. Spaulding and R. T. Disney, "Man-made radio noise, part 1: estimates for business, residential, and rural areas," Office of Telecommunications Report 74-38, Jun. 1974.
- [2] CCIR, "Man-made radio noise," Report 258-5, International Radio Consultive Committee, International Telecommunications Union, Geneva, Switzerland, 1990.
- [3] A.D. Spaulding, "The roadway natural and man-made noise environment," IVHS Journal, vol 2(2), pp. 175-211, 1995.
- [4] A.D. Spaulding, "The natural and man-made noise environment in personal communication services bands," NTIA Report 96-330 (revised), May 1997.
- [5] R. Dalke, R. Achatz, Y. Lo, P. Papazian, and G. Hufford, "Measurement and analysis of man-made noise in VHF and UHF bands," 1997 Wireless Communications Conference, Boulder, CO, August 11-13, 1997.
- [6] R. Achatz, Y. Lo, R. Dalke, G. Hufford and P. Papazian, "Man-made noise in the 136- to 138-MHz VHF Meteorological Satellite Band," NTIA Report in preparation.
- [7] Middleton, D. "Statistical-physical models of man-made and natural radio noise environments--Part I: First-order probability models of the instantaneous amplitude," Office of Telecommunications Report OT 74-36, Ap. 1974.
- [8] Middleton, D. "Statistical-physical models of man-made and natural radio noise environments--Part II: First-order probability models of the envelope and phase," Office of Telecommunications Report OT 76-86, Ap. 1976.
- [9] Middleton, D. "Statistical-physical models of man-made and natural radio noise environments--Part III: First-order probability models of the instantaneous amplitude of Class B interference," NTIA Contractor Report 78-1, Jun. 1978.
- [10] Middleton, D. "Statistical-physical models of man-made and natural radio noise environments--Part IV: Determination of the first-order parameters of Class A and Class B interference," NTIA Contractor Report 78-2, Sep. 1978.
- [11] G. H. Hagn, "Man-made radio noise and interference," in *Proc. Of AGARD Conf.*, No. 420, Lisbon, Portugal, Oct. 26-30, 1987, pp 5-1 to 5-15.
- [12] M. Abramowitz and I. A. Stegun, *Handbook of Mathematical Functions*, New York, NY: Dover Pub. Inc., 1972.
- [13] W. Weibull, "A statistical distribution function of wide applicability," *J. Appl. Mech.*, 18, pp 293-297, 1951.
- [14] M. C. Jeruchim, P. Balaban, and K. S. Shanmugan, *Simulation of Communication Systems*, Plenum Press, New York, 1992.

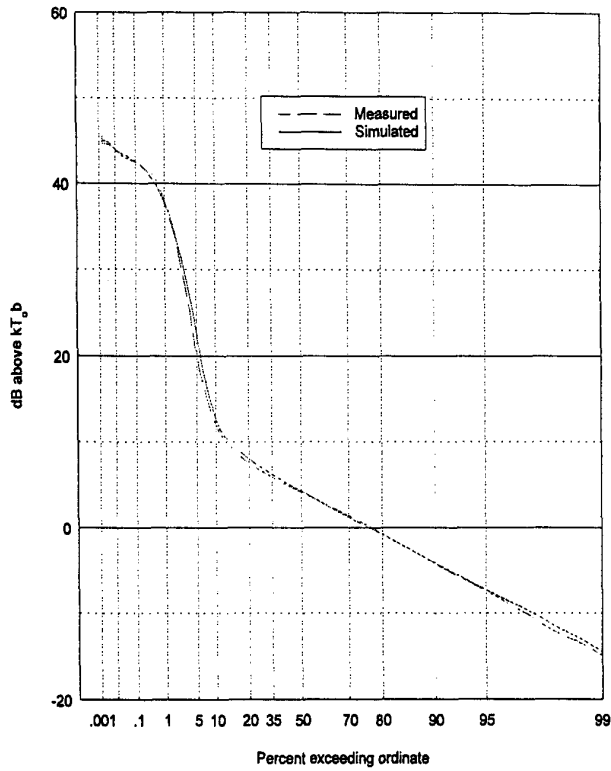


Figure 2. Class B noise near a rural power line.

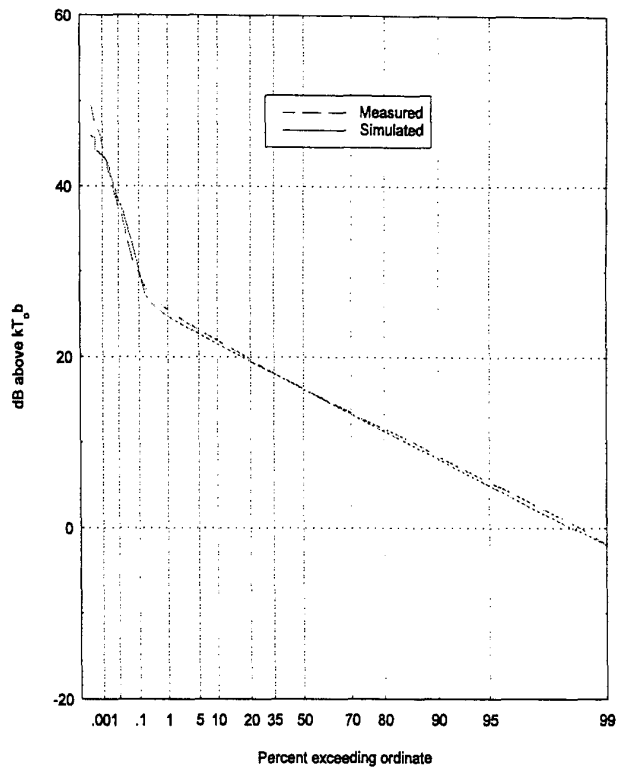


Figure 3. Class B in a downtown environment.

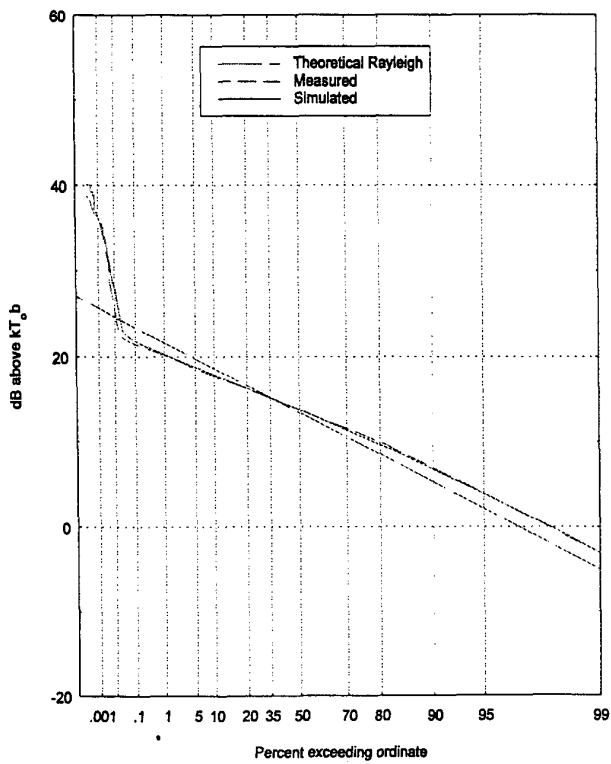


Figure 4. Class B noise in an office park environment.

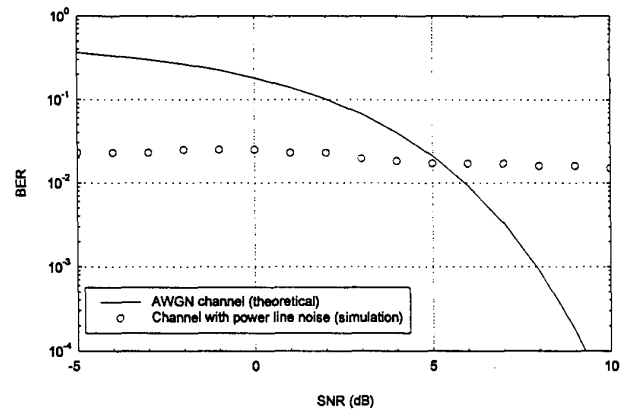


Figure 5. Simulated performance for DCBPSK modulation subjected to the power line noise process shown in Figure 2.